

Paramagnetic Particles Isolation of Influenza Oligonucleotide Labelled with CdS QDs

**Ludmila Krejцова, David Hynek, Pavel
Kopel, Vojtech Adam, Jaromir Hubalek,
Libuse Trnkova & Rene Kizek**

Chromatographia

An International Journal for Rapid
Communication in Chromatography,
Electrophoresis and Associated
Techniques

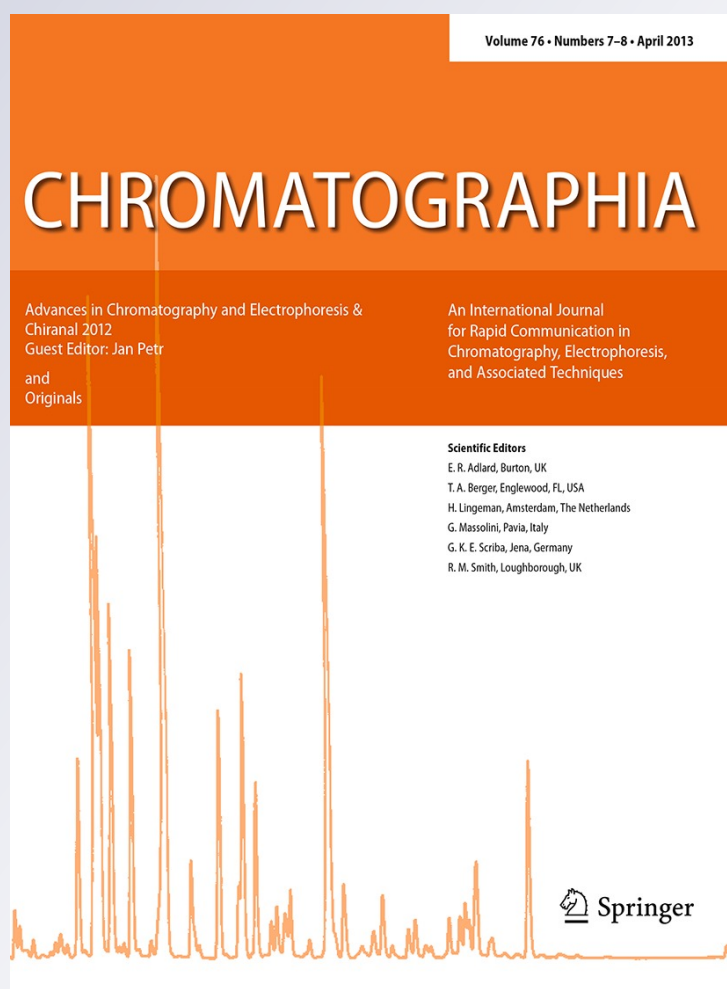
ISSN 0009-5893

Volume 76

Combined 7-8

Chromatographia (2013) 76:355-362

DOI 10.1007/s10337-012-2327-0



Your article is protected by copyright and all rights are held exclusively by Springer-Verlag. This e-offprint is for personal use only and shall not be self-archived in electronic repositories. If you wish to self-archive your work, please use the accepted author's version for posting to your own website or your institution's repository. You may further deposit the accepted author's version on a funder's repository at a funder's request, provided it is not made publicly available until 12 months after publication.

Paramagnetic Particles Isolation of Influenza Oligonucleotide Labelled with CdS QDs

Ludmila Krejcová · David Hýnek · Pavel Kopel ·
Vojtěch Adam · Jaromír Hubálek · Libuše Trnková ·
Rene Kizek

Received: 22 June 2012/Revised: 28 August 2012/Accepted: 30 August 2012/Published online: 4 October 2012
© Springer-Verlag 2012

Abstract In this study, we describe hybridization design probes consisting of paramagnetic particles and quantum dots (QDs) with targeted DNA, and their application for detection of avian influenza virus (H5N1). Optical properties of QDs were beneficial, but the main attention was paid to the electroactivity of metal part of QDs and ODNs themselves. Differential pulse voltammetry was used for detection of cadmium(II) ions and square wave voltammetry for detection of cytosine–adenine peak in ODN-SH-Cd complex. It clearly follows from the obtained results that the optimized conditions were temperature of hybridization 25 °C, time of hybridization 35 min, and concentration of ODN-SH-Cd complex 20 $\mu\text{g mL}^{-1}$. The detection limit (3 signal/noise) was estimated as 15 ng mL^{-1} of ODN-SH-Cd.

Keywords Biosensors · Voltammetry · Automated separation · Nanoparticles · Quantum dots · Hybridization · Virus

Introduction

Influenza is an infectious disease caused by RNA viruses of the family Orthomyxoviridae. Influenza viruses can be found in the aerosols formed by sneezing and coughing and may cause acute infection of upper respiratory tract [1, 2]. Vaccine against influenza exists; however, it is effective for one year against selected subtypes. This is due to mutational changes in the structure of the virus, thus the reuse of the same vaccine in the following year does not have a protected effect [3, 4]. It is clear that flu viruses are very susceptible to change antigenic equipment by drift and shift. These changes can easily create a new subtype, as in the case of highly pathogenic avian influenza. Owing to this, a great amount of research is being carried out in the search for rapid and more reliable detection methods [1, 5, 6].

Nucleic acid hybridization on solid bases is widely used in biotechnology for the isolation of targeted DNA. Among numerous methods used in this field, many probe–target DNA assays use oligo-conjugated paramagnetic particles (MPs) for the isolation of nucleic acids of interest [7, 8]. The advantage of magnetic separation is in the possibility of modifying the surface of MPs, and thus the elimination of interfering adsorption of non-target biomolecules [9–11], because MPs are able to respond to external magnetic field, which is used for efficient separation. Both magnetic separation and modification of MPs surfaces are beneficial for DNA isolation [12–14].

Isolated DNA is usually detected by hybridization process using different materials such as biotin–avidin, substrate

Published in the special paper collection *Advances in Chromatography and Electrophoresis & Chiral 2012* with guest editor Jan Petr.

L. Krejcová · D. Hýnek · P. Kopel · V. Adam · L. Trnková ·
R. Kizek (✉)
Department of Chemistry and Biochemistry,
Faculty of Agronomy, Mendel University in Brno,
Zemědělská 1, 613 00 Brno, Czech Republic
e-mail: kizek@sci.muni.cz

D. Hýnek · P. Kopel · V. Adam · J. Hubálek · L. Trnková ·
R. Kizek
Central European Institute of Technology,
Brno University of Technology, Technická 3058/10,
616 00 Brno, Czech Republic

J. Hubálek
Department of Microelectronics, Faculty of Electrical
Engineering and Communication, Brno University
of Technology, Technická 3058/10, 616 00 Brno, Czech Republic

enzyme, antigen–antibody and fluorescent dyes or other optical active substances as quantum dots (QDs) [15, 16], because detection of hybridized DNA molecule is important for diagnosis of the presence of specific virus [17]. Application of optical detection methods based on fluorescently active labels is widespread [18–20]. Recent advantages in synthesis and surface modifications of QDs as a new type of fluorescently active labels have resulted in various applications of these particles [21–25]. Wang et al. described multi-target electrochemical DNA detection based on the use of different QDs. Multi-target electrical detection scheme developed by those authors incorporates the high sensitivity and selectivity advantages of nanoparticle-based electrical assays [17]. It is clear that besides optical properties of these nanoparticles, QDs can be also used as electroactive labels for determination of biologically active compounds [26]. Therefore, one of the main aims of this study was the electrochemical detection of the presence of Cd and cytosine–adenine (CA) in H5N1 influenza derived oligonucleotide labelled with CdS. This detection part was coupled to paramagnetic particle-based isolation protocol as the second main aim of our study. The suggested procedure is shown in Fig. 1.

Experimental Section

Preparation of CdS QDs

All chemicals were purchased from Sigma-Aldrich (St. Louis, USA) and used without further purification. CdS QDs were prepared with a slightly modified method published in [27]. Cadmium nitrate tetrahydrate $\text{Cd}(\text{NO}_3)_2 \cdot 4\text{H}_2\text{O}$ (0.03085 g, 0.1 mM) was dissolved in ACS water (25 mL). 3-Mercaptopropionic acid (35 μL , 0.4 mM) was slowly added to stirred solution. Afterwards, pH was adjusted to 9.11 with 1 M NH_3 (1.5 mL). Sodium sulphide nanohydrate $\text{Na}_2\text{S} \cdot 9\text{H}_2\text{O}$ (0.02402 g, 0.1 mM) in 23 mL of ACS water was poured into the first solution with vigorous stirring. Obtained yellow solution was stirred for 1 h. CdS QDs were stored in dark at 4 °C. Fluorescence of the obtained QDs is shown in Fig. 2. We found that the synthesized objects were smaller than 10 nm.

Preparation of CdS Labelled H5N1 Influenza Oligonucleotide (ODN-SH-Cd)

ODN-SH H5N1 5'-SH-CTTCTTCTCTCTCCTTGAGG-3' (100 μL , 100 $\mu\text{g mL}^{-1}$) was mixed with a solution of CdS QDs (100 μL). This mixture was shaken for 24 h at room temperature using Vortex Genie2 (Scientific Industries, New York, USA). Subsequently, solution was dialysed against 2,000 mL of milli Q water (24 h, 4 °C) on Millipore

membrane filter 0.025 μm VSWP. During dialysis, the sample was diluted to 800 μL . Diluted sample was concentrated to 500 μL final volume on a centrifugal filter device Amicon Ultra 3k (Millipore, Billerica, USA). Centrifuge 5417R (Eppendorf, Hamburg, Germany) was utilized with following parameters 15 min, 4,500 rpm, 15 °C.

Robotic Pipetting Station

For automated samples handling before their electrochemical analysis, an automated pipetting station ep-Motion 5075 (Eppendorf) with computer controlling was used. Positions C1 and C4 were thermostated (Eptermo-adaptor PCR96). In B1 position, module reservoir for washing solutions and waste were placed. Tips were placed in positions A4 (epTips 50), A3 (epTips 300) and A2 (epTips 1000). Transfer was ensured by a robotic arm with pipetting adaptors (TS50, TS300, TS1000) numeric labeling refers to maximal pipetting volume in μL and a gripper for platforms transport (TG-T). The program sequence was edited and the station was controlled in pEditor 4.0. For sample preparation, two platforms were used: Thermorack for 24 \times 1.5–2 mL microtubes (position C3), which was used for storage of working solutions, 96-well microplate with well volume of 200 μL (position C1), which was thermostated. After the separation, the MPs were forced using Promega magnetic pad (Promega, Madison, USA) (position B4) and the solutions were transferred to a new microplate.

Automatic Isolation of ODN-SH-Cd

Automatic pipetting station ep-Motion 5075 (Eppendorf) with original devices was used for fully automated influenza-derived oligonucleotide isolation process. The buffers used in isolation part of experiment were as follows: phosphate buffer I: 0.1 M NaCl + 0.05 M Na_2HPO_4 + 0.05 M NaH_2PO_4 ; phosphate buffer II: 0.2 M NaCl + 0.1 M Na_2HPO_4 + 0.1 M NaH_2PO_4 ; and hybridization solution: 100 mM Na_2HPO_4 + 100 mM NaH_2PO_4 , 0.5 M NaCl, 0.6 M guanidium thiocyanate, 0.15 M Trizma base adjusted by HCl on pH of 7.5.

The protocol was as follows: 10 μL of Dynabeads Oligo (dT)₂₅ (1 μm diameter, Hämeenlinna, Finland) was dispensed in each well in the plate (PCR 96, Eppendorf). Plate was subsequently transferred to the magnet, stored solution from nanoparticles was aspirated to waste, and beads were further washed three times with 20 μL of phosphate buffer I. The next step was *first hybridization*. 10 μL of polyA-modified anti-sense H5N1 oligonucleotide and 10 μL of hybridization buffer (0.1 M phosphate buffer, 0.6 M guanidium thiocyanate, 0.15 M Tris) were added into each

Fig. 1 Scheme of H5N1 (ODN-SH-Cd) isolation and electrochemical detection. **a** Anti-H5N1 binding to MP due to A-T complementarity, **b** addition of ODN-SH-Cd, **c** binding of ODN-SH-Cd to MP with anti-H5N1 and **d** electrochemical detection of ODN and Cd

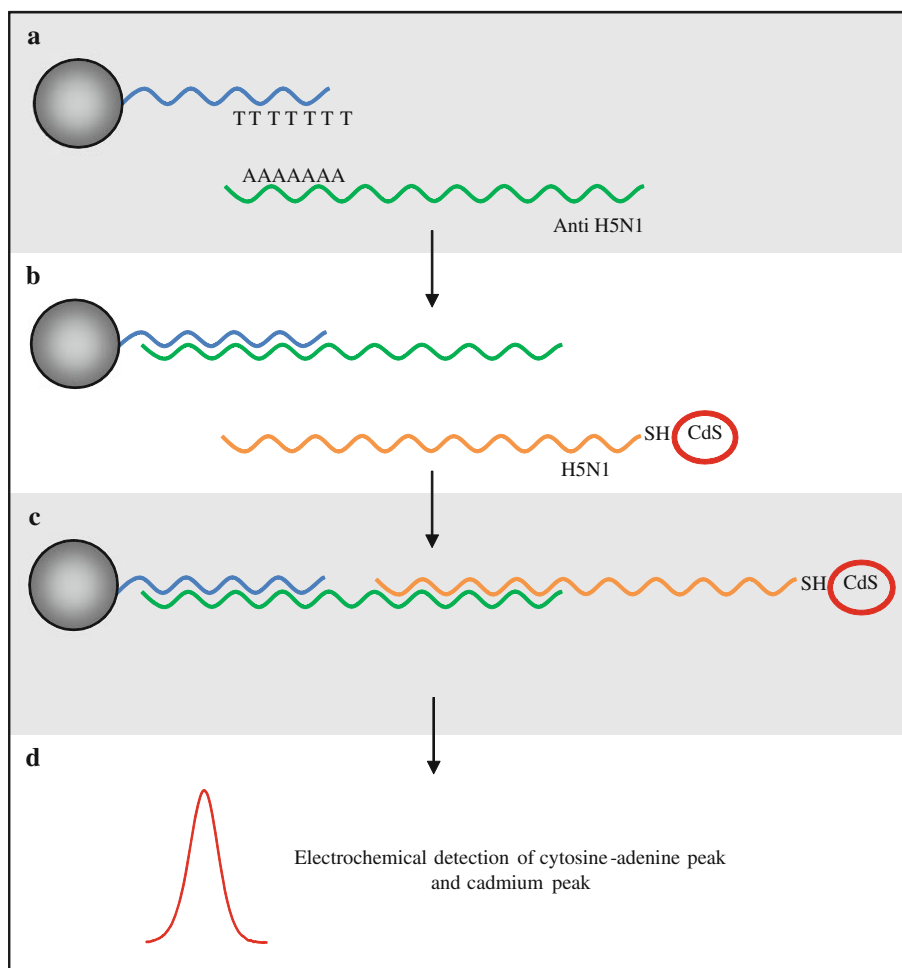
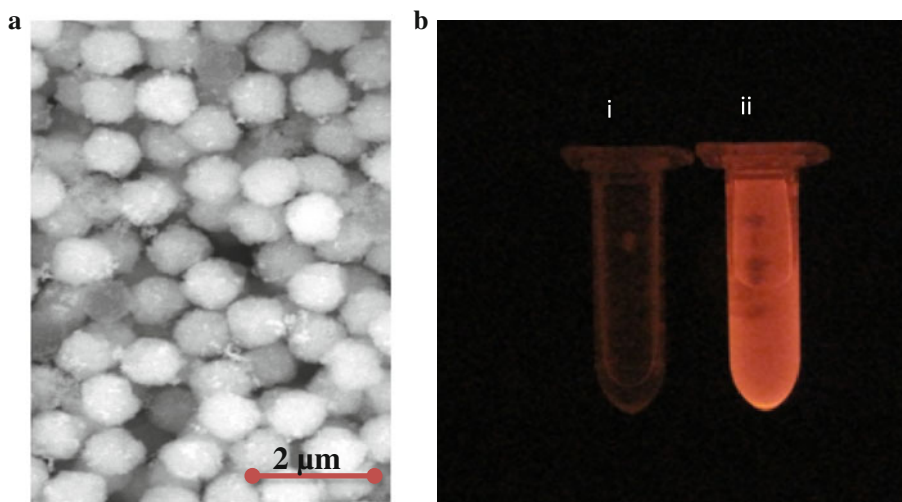


Fig. 2 a SEM micrograph of paramagnetic particles modified with dT25 (SEM HV 15.0 kV). **b** CdS QDs (i) without UV light, (ii) UV light 305 nm. The fluorescence was monitored by in vivo Xtreme system by Carestream, Woodbridge, USA. This instrument was equipped with 400 W xenon light source and 28 excitation filters (410–760 nm). The emitted light was captured by 4 MP CCD camera



well. Further, the plate was incubated (15 min, 25 °C, pipetting), followed by three times washing with 20 μL phosphate buffer I. The next step was *second hybridization*. 10 μL of Cd labelled H5N1 oligonucleotide and 10 μL of hybridization buffer (0.1 M phosphate buffer, 0.6 M guanidium thiocyanate, 0.15 M Tris) were added to each well,

and the plate was incubated (15 min, 25 °C, pipetting), followed by three times washing with 20 μL of phosphate buffer I. Afterwards, 30 μL of elution solution (phosphate buffer II) was added into each well, and the plate was incubated (5 min, 85 °C, pipetting). After elution step, the plate was transferred to the magnet, and product from each

well was transferred to separate well. The whole procedure was optimized by other authors [28–30].

Methods for Detection of CA and Cd Peak (ODN-SH-Cd)

Measurements were performed at 663 VA Stand, 800 Dosino and 846 Dosing Interface (Metrohm, Zofingen, Switzerland) using a standard cell with three electrodes. A hanging mercury drop electrode with a drop area of 0.4 mm² was employed as the working electrode. An Ag/AgCl/3 M KCl electrode served as the reference electrode, while the auxiliary electrode was a glassy carbon electrode. All measurements were performed in the presence of 0.2 M acetate buffer (0.2 M CH₃COOH + 0.2 M CH₃COONa, pH 5.0) at 25 °C. Samples were deoxygenated by argon (99.99 %, 120 s). For smoothing and baseline correction, the software GPES 4.9 supplied by EcoChemie (Utrecht, Netherlands) was employed. For detection of DNA, CA peak measured by square wave voltammetry (SWV) was used. The parameters of electrochemical determination were as follows: initial potential 0 V; end potential –1.85 V; frequency 10 Hz; potential step 0.005 V; and amplitude 0.025 V. For electrochemical detection of cadmium (Cd peak), differential pulse voltammetry (DPV) was used. The parameters of electrochemical determination were as follows: initial potential –0.9 V; end potential –0.45 V; deposition potential –0.9 V; duration 240 s; equilibration time 5 s; modulation time 0.06; time interval 0.2 s; potential step 0.002 V; and modulation amplitude 0.025.

Scanning Electron Microscope

A modern scanning electron microscope (SEM) with motorized stage, full software control and image acquisition was recognized as a relatively easy way for automated high-resolution documentation of particles. For each experiment, three independent samples of particles on different tablet sections (glass, pure Si, and Millipore syringe filters) were documented. FEG-SEM TESCAN MIRA 3 XMU (Brno, Czech Republic) was used for documentation. This model is equipped with a high brightness Schottky field emitter for low noise imaging at fast scanning rates. The SEM was fitted with Everhart–Thronley type of SE detector, high speed YAG scintillator-based BSE detector and panchromatic CL Detector.

Descriptive Statistics

Data were processed using MICROSOFT EXCELS (USA) and STATISTICA.CZ Version 8.0 (Prague, Czech Republic). The results are expressed as mean ± SD unless noted otherwise. The detection limits (3 signal/noise, S/N)

were calculated according to Long and Winefordner [31], whereas N was expressed as standard deviation of noise determined in the signal domain unless stated otherwise.

Results and Discussion

Rapid detection of the presence of virus represents a challenge for modern bioanalytical chemistry. For this purpose, MPs bring many advantages including possibility of miniaturization of the instrument as lab-on-chip [28]. Moreover, paramagnetic particles are suitable for sensing, therapeutic and diagnostic purposes [32]. In this study, particles modified with short thymine chain (dT25) were used (Fig. 2a). Next step was labelling of influenza derived thiolated oligonucleotide with CdS QDs. These QDs were prepared from cadmium nitrate tetrahydrate according to procedure mentioned in the “Experimental” section. The prepared CdS QDs had fluorescent properties as shown in Fig. 2b. The possibilities of labelling of nucleic acids and proteins with QDs are discussed by Joseph Wang and Cliphord Mirkin and showed many advantages for potential applications in nanomedicine [33–37]. The last part of preparation of sensing assay was full automation of the isolation with subsequent electrochemical detection of CdS labelled H5N1 influenza derived oligonucleotide (ODN-SH-Cd). Scheme of ODN-SH-Cd isolation and electrochemical detection is shown in Fig. 1.

Determination of Cadmium(II) Ions and ODNs

For the quantification of the interactions between CdS QDs and ODNs, determination of the presence of the formed complex via electrochemical detection of cadmium(II) ions is very advantageous, because electroanalysis of metal ions is well known, sensitive, and robust enough to be used routinely for analysis of various types of real samples [38, 39]. DPV was used for detection of cadmium(II) ions in CdS QDs. Peak of cadmium(II) ions enhanced with the increasing accumulation time up to 300 s, which was selected as the optimum for the following experiments (Fig. 3a). The obtained CdS QDs concentration dependence was linear within the range from 0.5 to 70 µg mL⁻¹ as it follows $y = 0.6473x$; $R^2 = 0.9990$, $n = 5$, RSD = 2.1 % (Fig. 3b). If cadmium(II) ions (CdS) were detected in bounded forms with ODNs, then well-developed peaks of Cd(II) were measured at -0.58 ± 0.02 V ($n = 5$). Determined calibration dependence was following $y = 20.64x$; $R^2 = 0.9941$, $n = 5$, RSD = 3.8 % (Fig. 3c). The limit of detection (3 S/N) was determined as 1 ng mL⁻¹ ODN-SH-Cd.

For the complete characterization of system, we needed electrochemical determination of ODNs. SWV was selected for this purpose. ODN-SH (full line) and ODN-

SH–Cd (dotted line) complex provided various SWV records (Fig. 4a). For ODN-SH characteristic, CA peak was detected at -1.348 ± 0.005 V). Oligonucleotide ODN-SH-Cd showed two peaks. The first one corresponded to cadmium(II) ions (Cd peak, -0.58 ± 0.005 V), and the second one to the nucleic acid (CA peak, -1.362 ± 0.002 V). There were also significant differences between CA peaks of Cd labelled and non-labelled oligonucleotides. Non-labelled ODN gave higher and thinner CA peak

compared with ODN-SH-Cd. Slight difference in the CA peak position was determined (QDs labelled: -1.362 V and non-labelled: -1.348 V). The only difference between these oligonucleotides is the bound CdS to the 5' SH end of influenza derived oligonucleotide. It follows that the change of the CA signal must be caused by QDs binding, but effect of CDs on the CA peak is not fully understood, but the changes can be associated with changes of electric properties of nucleic acids [40].

After characterization of labelled and non-labelled ODNs, the optimization of accumulation times for both ODNs was done. Binding of CdS to ODN-SH decreased CA peak in the whole tested interval, but in both cases, the value of 120 s was selected as optimal for further studies

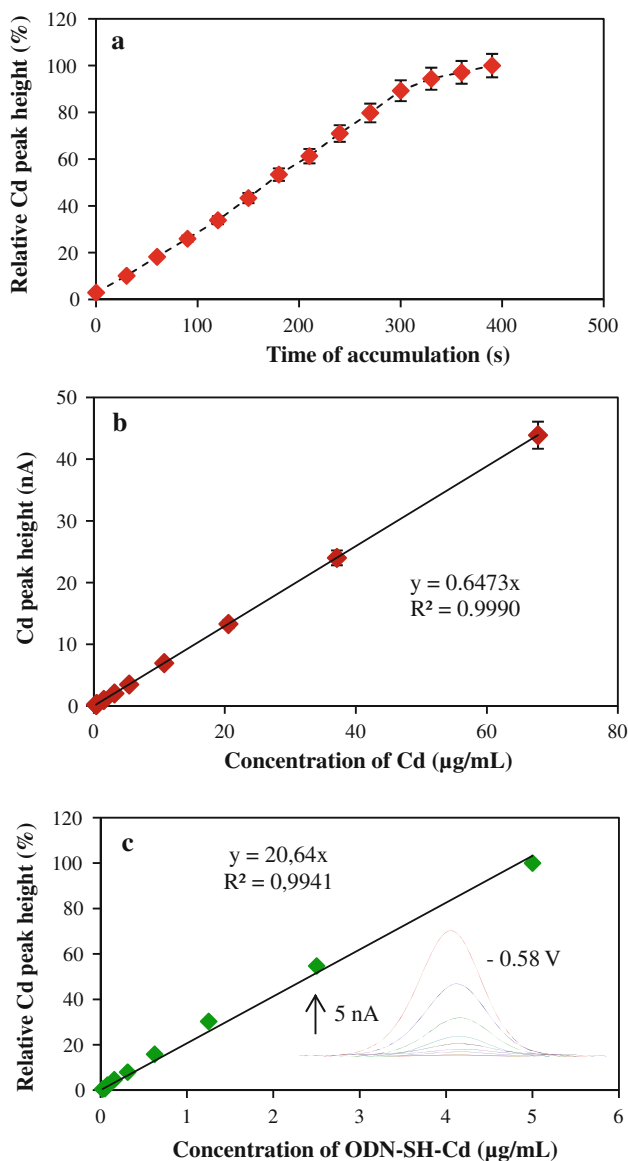


Fig. 3 **a** Optimization of time of accumulation for Cd(II) determination by DPV with parameters as follows: initial potential -0.9 V; end potential -0.45 V; deposition potential -0.9 V; duration 240 s; equilibration time 5 s; modulation time 0.06; time interval 0.2 s; potential step 0.002 V; and modulation amplitude 0.025. **b** Obtained calibration curve for Cd(II) ions. **c** Cadmium was determined in ODN-SH-Cd complex too. Dependence of cadmium signal (peak height) on concentration of complex is presented

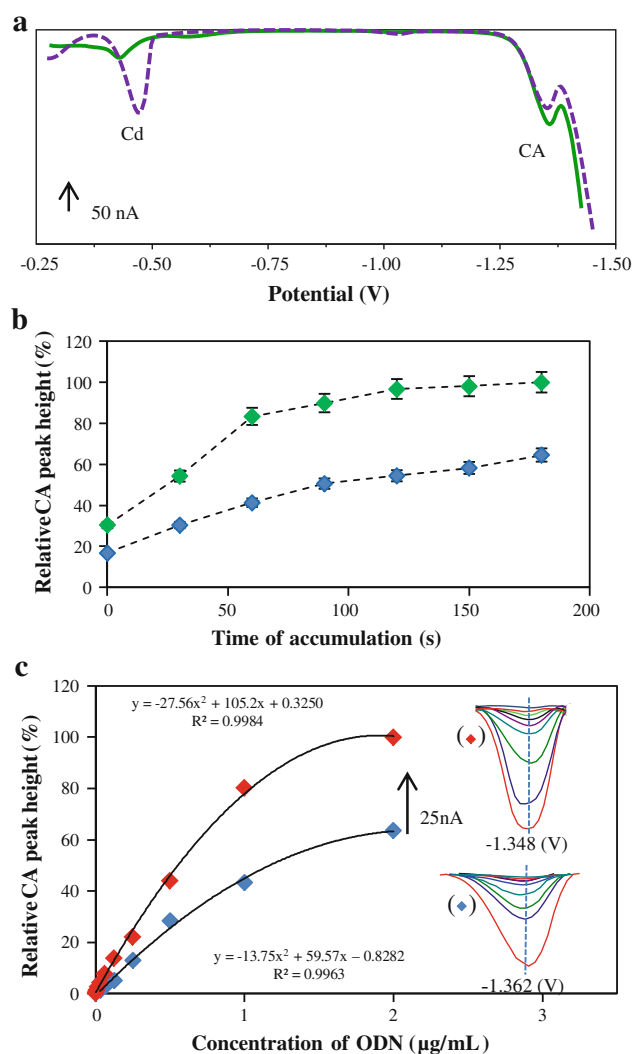


Fig. 4 **a** Comparison of typical SW voltammograms of ODN-SH (full line) and ODN-SH-Cd (dotted line). **b** Dependence of CA peaks of ODN-SH (green diamonds) and ODN-SH-Cd (blue diamonds) on accumulation time. **c** Calibration curves CA peaks of (red diamonds) ODN-SH and (blue diamonds) ODN-SH-Cd. Start concentration of both ODNs was $2 \mu\text{g mL}^{-1}$. CA peak was measured by SWV

(Fig. 4b). Dependences of CA peak height on both labelled and non-labelled ODN concentrations are shown in Fig. 4c. It is shown that the both dependences have polynomial calibration equations. For ODN-SH, the equation was $y = -27.56x^2 + 105.2x + 0.3250$; $R^2 = 0.9984$, $n = 5$, RSD = 3.2 and for ODN-SH-Cd $y = -13.75x^2 + 59.57x - 0.8282$; $R^2 = 0.9963$, $n = 5$, RSD = 2.9. The detection limits (3 S/N) were estimated as 15 ng mL^{-1} of ODN-SH-Cd and 30 ng mL^{-1} of ODN-SH.

Optimization of Separation Process: Hybridizations

Paramagnetic particles (MPs) are able to respond to external magnetic field, which is used for efficient separation of different analytes from liquid samples. Isolation of biomolecules using MPs is usually followed by electrochemical detection. This way of isolation and detection is less time-consuming and it is highly sensitive to even small quantities of sample [28, 41]. In order to study using MPs as a tool for hybridization assays we designed a MP- and QD-based hybridization assay for the detection of avian influenza H5N1, respectively H5N1-derived oligonucleotide. Figure 1 shows a schematic view of the hybridization procedure for isolation and detection of target (ODN-SH-Cd). The separation procedure contains from four items arranged in the following order: (i) polyA-modified oligo probes (oligo anti-sense) bind on the surface of polyT MPs due to specific TA capturing, (ii) Cd QDs labelling target oligonucleotide, (iii) capturing of target QDs labelled oligonucleotide derived from an influenza sequence, and (iv) electrochemical detection of metal part of QDs marker by DPV. Electrochemical detection of influenza H5N1-derived oligonucleotide using SWV was connected too.

Based on the above mentioned results it can be concluded that CdS QDs can be used for detection of specific ODNs labelled with CdS QDs. Therefore, we were interested in the issue how we can affect the optimize isolation process. We aimed our attention to second hybridization, where the binding of target molecule on the modified MPs takes place. The hybridization process is influenced by wide range of hybridization conditions such as temperature, time, mixing, pH and composition of hybridization buffer. For the first step we aimed our attention to the temperature of hybridization process. The hybridization process was repeated four times under these temperatures of 15, 20, 25 and 30 °C. At the end of hybridization process, peaks of ODN (CA peak) and signals of Cd(II) ions (Cd peak) were determined. Measured peak height was recalculated with respect to the amount of ODN-SH-Cd molecules for both determined signals (Fig. 5a, b). It is evident that increasing temperature enhanced effectiveness of hybridization and thus CA and Cd peak heights. The most effective hybridization was carried out under 25 °C.

This temperature is more effective than 30 °C, because T_m of influenza-derived oligonucleotide is 28 °C.

Second hybridization parameter, which was optimized, was time of hybridization. The obtained results show that peak heights of ODN and Cd(II) enhanced with the increasing time of hybridization (Fig. 6a). Response of Cd signal increased linearly within the range from 5 to 35 min as it follows $y = 1.970x + 31.23$; $R^2 = 0.9991$, $n = 3$, RSD = 4.8. In contrast, the ODN signal (CA peak) was changed quadratically as it follows $y = 0.1266x^2 - 1.945x + 11.52$; $R^2 = 0.9926$, $n = 3$, RSD = 5.1.

The third changing condition of hybridization process was concentration of ODN-SH-Cd complex. The concentration was changed within the interval from 2.5 to $20 \mu\text{g mL}^{-1}$ and both CA and Cd peaks were determined (Fig. 6b). As for previous parameters, the concentration of ODN-SH-Cd complex influenced measured peaks in the same way. Response of Cd peak increased linearly as it follows $y = 2.202x + 56.61$; $R^2 = 0.9958$, $n = 3$, RSD = 3.8, and ODN peak quadratically as it follows $y = -0.2013x^2 + 7.412x + 32.04$; $R^2 = 0.9838$, $n = 3$, RSD = 5.6 with the increasing concentration of ODN-SH-Cd

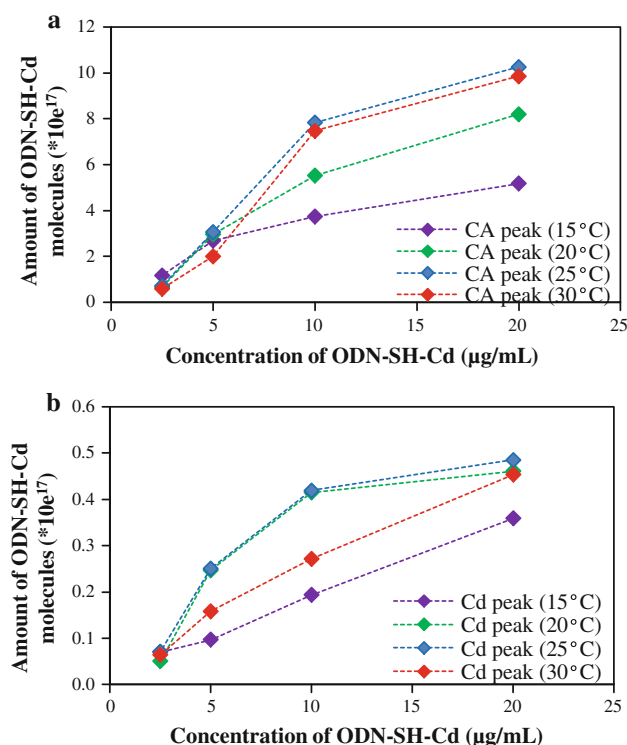


Fig. 5 **a** Detected amount of ODN-SH-Cd molecules ($\times 10^{17}$) as a function of start concentration of ODN-SH-Cd ($\mu\text{g mL}^{-1}$) after separation process referenced for CA peak. **b** Amount of ODN-SH-Cd molecules ($\times 10^{17}$) as a function of start concentration of ODN-SH-Cd ($\mu\text{g mL}^{-1}$) referenced for Cd peak. CA peak was measured by SWV and Cd peak by DPV. First hybridization step was carried out for 30 min at 25 °C

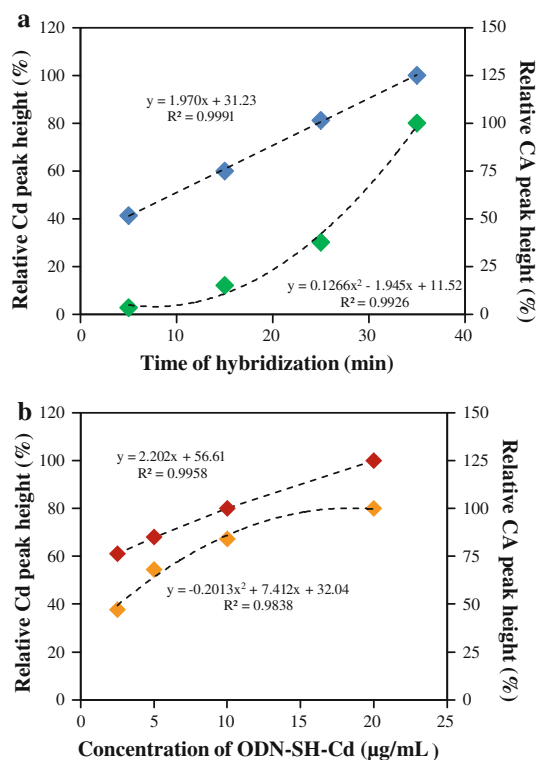


Fig. 6 **a** Change of relative peak height (relate to maximum value of CA and Cd peak) with the increasing of time of second hybridization (5, 15, 25 and 35 min). (Green diamonds) Change of CA peak (determined by SWV) and (blue diamonds) of Cd peak (determined by DPV). **b** Dependence of relative peak height (relate to maximum value of CA and Cd peak) on concentration of ODN-SH-Cd complex (2.5, 5, 10 and 20 $\mu\text{g mL}^{-1}$) at 25 °C. (Orange diamonds) Change of CA peak (determined by SWV) and (red diamonds) of Cd peak (determined by DPV)

complex. It clearly follows from the obtained results that the optimized conditions were temperature of hybridization 25 °C, time of hybridization 35 min and concentration of ODN-SH-Cd complex 20 $\mu\text{g mL}^{-1}$. Under these conditions, we can obtain the best efficiency in isolation and detection of influenza oligonucleotide.

The obtained results show that suggested method of isolation and detection of Cd labelled influenza-derived oligonucleotide is functional and provide electrochemically measurable signal of target molecule. Cd peak gives us the information about successful hybridization process, and ODN peak relates with the presence of ODNs in solution after hybridization process. The number of molecules determined from CA peak is approximately ten times higher than the number from Cd peak. This effect might be explained from breakage of creating complex after second hybridization in the other place that we assumed. Based on our previously published articles, the breakage of complex can proceed at A-T place [28–30]. We assumed that this situation can be explained from binding of more

oligonucleotides to one CdS QD particle. This reasoning is in accordance with studies of Nolan et al. [42] and Ho et al. [43] who reported the use of QDs labelling oligo probes for hybridization with target DNA. Yet another published study is based on DNA-cross-linked CdS nanoparticles array [44] and shows similar effect.

Conclusion

Nowadays, research is directed towards finding methods for simultaneous detection of multiple DNA targets. The electrochemical coding technology is thus expected to open up new opportunities for DNA diagnostics [17, 45]. In this study, an optimized method for automated isolation of Cd-labelled influenza oligonucleotide using automated pipetting station has been proposed. The effects of hybridization temperature, hybridization time, and concentration of ODN-SH-Cd complex on CA and Cd peak height, which were determined electrochemically using SWV and DPV, were also demonstrated. The system proposed in this study can be used as electroanalytical tool for rapid detection of target oligonucleotide based on isolation by probe conjugated MPs.

Acknowledgments Financial support from the projects NANIMEL GA CR 102/08/1546 and CEITEC CZ.1.05/1.1.00/02.0068 is gratefully acknowledged.

References

1. Peiris JSM, Poon LLM, Guan Y (2012) *Science* 335:1173–1174
2. Osterholm MT, Henderson DA (2012) *Science* 335:801–802
3. Feng ZL, Towers S, Yang YD (2011) *AAPS J* 13:427–437
4. Ghendon Y (1994) *Eur J Epidemiol* 10:451–453
5. Fouchier RAM, Herfst S, Osterhaus A (2012) *Science* 335:662–663
6. Karlas A, Machuy N, Shin Y, Pleissner KP, Artarini A, Heuer D, Becker D, Khalil H, Ogilvie LA, Hess S, Maurer AP, Muller E, Wolff T, Rudel T, Meyer TF (2010) *Nature* 463:818–822
7. Elghanian R, Storhoff JJ, Mucic RC, Letsinger RL, Mirkin CA (1997) *Science* 277:1078–1081
8. Katz E, Willner I (2004) *Angew Chem Int Ed* 43:6042–6108
9. Hsing IM, Xu Y, Zhao WT (2007) *Electroanalysis* 19:755–768
10. Drbohlavova J, Hrdy R, Adam V, Kizek R, Schneeweiss O, Hubalek J (2009) *Sensors* 9:2352–2362
11. Pumera M (2011) *Chem Commun* 47:5671–5680
12. Ahmed ARH, Olivier GWJ, Adams G, Erskine ME, Kinsman RG, Branch SK, Moss SH, Notarianni LJ, Pouton CW (1992) *Biochem J* 286:377–382
13. Ossendorp FA, Bruning PF, Vandenbrink JAM, Deboer M (1989) *J Immunol Methods* 120:191–200
14. Xu HX, Sha MY, Wong EY, Uphoff J, Xu YH, Treadway JA, Truong A, O'Brien E, Asquith S, Stubbins M, Spurr NK, Lai EH, Mahoney W (2003) *Nucleic Acids Res* 31:e43
15. Lim SH, Bestvater F, Buchy P, Mardy S, Yu ADC (2009) *Sensors* 9:5590–5599
16. Hicks JM (1984) *Hum Pathol* 15:112–116

17. Wang J, Liu GD, Merkoci A (2003) *J Am Chem Soc* 125:3214–3215
18. Cao YWC, Jin RC, Mirkin CA (2002) *Science* 297:1536–1540
19. Taton TA, Mirkin CA, Letsinger RL (2000) *Science* 289:1757–1760
20. Nicewarner-Pena SR, Freeman RG, Reiss BD, He L, Pena DJ, Walton ID, Cromer R, Keating CD, Natan MJ (2001) *Science* 294:137–141
21. Bakalova R, Zhelev Z, Ohba H, Baba Y (2005) *J Am Chem Soc* 127:11328–11335
22. Agrawal A, Sathe T, Nie SM (2007) *J Agric Food Chem* 55:3778–3782
23. Peterson AW, Heaton RJ, Georgiadis RM (2001) *Nucleic Acids Res* 29:5163–5168
24. Steel AB, Levicky RL, Herne TM, Tarlov MJ (2000) *Biophys J* 79:975–981
25. Ryvolova M, Chomoucka J, Janu L, Drbohlavova J, Adam V, Hubalek J, Kizek R (2011) *Electrophoresis* 32:1619–1622
26. Krejcová L, Dospivová D, Ryvolova M, Kopel P, Hyněk D, Krizkova S, Hubalek J, Adam V, Kizek R (2012) *Electrophoresis*. doi:10.1002/elps.201200304
27. Li H, Shih WY, Shih WH (2007) *Ind Eng Chem Res* 46:2013–2019
28. Adam V, Huska D, Hubalek J, Kizek R (2010) *Microfluid Nanofluid* 8:329–339
29. Huska D, Hubalek J, Adam V, Vajtr D, Horna A, Trnkova L, Havel L, Kizek R (2009) *Talanta* 79:402–411
30. Janicek Z, Huska D, Trnkova L, Provaznik I, Hubalek J, Kizek R (2010) *J Biochem Technol* 2:S87–S88
31. Long GL, Winefordner JD (1983) *Anal Chem* 55:A712–A724
32. Huska D, Adam V, Trnkova L, Kizek R (2009) *J Magn Magn Mater* 321:1474–1477
33. Ju HX, Zhang XJ, Wang J (2011) In: *Nanobiosensing: principles, development and application*. Springer, New York, pp 535–567
34. Nam JM, Park SJ, Mirkin CA (2002) *J Am Chem Soc* 124:3820–3821
35. Nam JM, Thaxton CS, Mirkin CA (2003) *Science* 301:1884–1886
36. Rosi NL, Mirkin CA (2005) *Chem Rev* 105:1547–1562
37. Wang J (2009) *ACS Nano* 3:4–9
38. Huska D, Zitka O, Krystofova O, Adam V, Babula P, Zehnalek J, Bartusek K, Beklova M, Havel L, Kizek R (2010) *Int J Electrochem Sci* 5:1535–1549
39. Kleckerova A, Sobrova P, Krystofova O, Sochor J, Zitka O, Babula P, Adam V, Docekalova H, Kizek R (2011) *Int J Electrochem Sci* 6:6011–6031
40. Slinker JD, Muren NB, Renfrew SE, Barton JK (2011) *Nat Chem* 3:228–233
41. Halfpenny KC, Wright DW (2010) *Wiley Interdiscip Rev Nanomed Nanobiotechnol* 2:277–290
42. Nolan RL, Cai H, Nolan JP, Goodwin PM (2003) *Anal Chem* 75:6236–6243
43. Ho YP, Kung MC, Yang S, Wang TH (2005) *Nano Lett* 5:1693–1697
44. Willner I, Patolsky F, Wasserman J (2001) *Angew Chem Int Ed* 40:1861–1864
45. Chomoucka J, Drbohlavova J, Masarik M, Ryvolova M, Huska D, Prasek J, Horna A, Trnkova L, Provaznik I, Adam V, Hubalek J, Kizek R (2012) *Int J Nanotechnol* 9:746–783